Adaptive sliding-mode torque control of a PM synchronous motor

C.-H. Fang, C.-M. Huang and S.-K. Lin

Abstract: An adaptive sliding-mode torque control system, which incorporates the merits of both the sliding-mode control and the adaptive algorithm, is proposed. The sliding-mode controller is constructed by two integral surface functions. The uncertainty is formulated as a random variable around a constant mean, so that an adaptive mechanism is used to estimate the constant mean and the bound of the random variable. Moreover, an application of the proposed torque control to the position control of a motor is also presented. Some experiments verify the control theory and demonstrate the usefulness of the proposed control scheme.

1 Introduction

Permanent magnetic synchronous motors (PMSM) are receiving increased attention for drive applications ranging from high-performance servo drives to line-start applications such as fans and pumps. The main reasons are their high power density, large torque to inertia ratio, high efficiency, and the falling prices of high-energy magnets [1].

The main earlier methods for PMSM control are based on current control techniques, e.g., vector control [2], predictive control [3], and others [4–6]. The torque in PMSMs is usually controlled by controlling the armature current based on the fact that electromagnetic torque is proportional to the armature current. For high performance, the current control is normally executed in the rotor dq-reference frame which rotates with the rotor. Therefore, coordinate transformation is involved. The torque response under this type of control is limited by the time constant of motor winds [7].

Rotor field-oriented (RFO) control for PMSM [5, 6] drives provides the decoupling control between the torque and flux components, and can achieve good performance characteristics similar to that of a DC motor, so RFO control is a popular control method for PMSM. The drawback of the RFO is that it uses a linear PI controller to handle the nonlinear system. Thanks to the high gain, the RFO performs well in most cases. But in worse cases (e.g., at a moderately high speed), the performance of RFO could be improved by using nonlinear control. According to the frequency response theory of linear systems, the PI controller will have a lag phenomenon in the sinusoid response for an appropriate frequency, even if the controlled plant is a first-order linear system.

The current trend is then to develop a nonlinear controller for a PMSM, especially using torque control laws [7–9]. Direct torque control (DTC) is one method of increasing interest in recent years. The basic principle of DTC is to directly select the stator voltage vector according to the differences between the references of torque and stator flux and their actual values [10]. The advantages of DTC are a quick torque response and lesser parameter dependence. However, torque ripples and high sample time are drawbacks. On the other hand, feedback linearisation control can be successfully applied to the PMSM torque control [11, 12]. However, it requires the precise values of the system parameters.

Over the past decade, variable structure control strategy using a sliding-mode has been the focus of much research into the control of the AC drive system [13–17]. The key objective of this technique is to force the system trajectory to a specific surface, known as the sliding surface, such that the state variables of the system are totally determined by the sliding surface. The main feature of the approach is its insensitivity to disturbances and parameter variations.

This paper presents an adaptive sliding-mode torque control for a PMSM. The stator voltage command is directly generated from the torque and flux errors based on two integral sliding surface functions. As in usual sliding-mode control, the asymptotic stability of the proposed control law can be shown by the Lyapunov method. Moreover, an adaptive inference mechanism with adaptation of the nominal uncertainty and the maximum offset value is included, which follows from the concept of the adaptive sliding-mode control [16]. Furthermore, we propose a cascade control system to apply the sliding-mode torque control to the position control of a PMSM. The overall control system consists of the inner loop of the torque control and the outer loop of the position control. The position control is designed using model reference adaptive control (MRAC). Some experiments are provided to verify the control system.

2 Model of a PMSM

The model of a surface-mounted PMSM in the synchronous rotor-rotating reference frame (d, q) can be described as [6, 18]:

$$\dot{i}_{ds} = -\frac{R_s}{L_s} i_{ds} + p\omega_r i_{qs} + \frac{u_{ds}}{L_s} \tag{1}$$

IEE Proceedings online no. 20020071

DOI: 10.1049/ip-epa:20020071

Paper first received 2nd August 2001 and in revised form 13th December 2001

The authors are with the Department of Electrical and Control Engineering, National Chiao Tung University, 1001 Ta Hsueh Road, Hsinchu 30010, Taiwan

$$\dot{i}_{qs} = -\frac{R_s}{L_s} i_{qs} - p\omega_r i_{ds} - \frac{p\omega_r}{L_s} K_f + \frac{u_{qs}}{L_s} \tag{2}$$

$$\dot{\omega}_r = -\frac{B}{J}\omega_r + \frac{T_e}{J} + \frac{T_L}{J} \tag{3}$$

where R_s is the stator resistance, L_s is the stator inductance, K_f is the armature (or stator) back EMF constant, B and J are the friction coefficient and the moment of inertia of the motor, p is the number of pole-pairs, ω_r is the rotor speed, (i_{ds}, i_{qs}) and (u_{ds}, u_{qs}) are, respectively, stator currents and voltages in the rotor-rotating frame (d, q), and T_e and T_L are the electromagnetic torque and external load torque. Note that

$$T_e = \mu(i_{qs}\varphi_{ds} - i_{ds}\varphi_{qs}) \tag{4}$$

where $\mu \equiv 3p/2$, and (φ_{ds}, φ_{qs}) are the stator fluxes in the form of

$$\varphi_{ds} = L_s i_{ds} + K_f \tag{5}$$

$$\varphi_{qs} = L_s i_{qs} \tag{6}$$

3 Adaptive sliding-mode torque control

We want to propose a direct torque control scheme for a PMSM, which tracks the electromagnetic torque T_e by controlling the voltage inputs to the motor. It is known that the squared norm of the stator fluxes is closely related to electromagnetic torque. We then need to take into account the active torque (u_T) as well as the square of the flux norm (u_ϕ). Both are defined as follows:

$$u_T = i_{qs}\varphi_{ds} - i_{ds}\varphi_{qs} \tag{7}$$

$$u_\phi = (\varphi_{ds}^2 + \varphi_{qs}^2)/2 \tag{8}$$

(7) and (8) require the signals of i_{ds}, i_{qs}, φ_{ds}, and φ_{qs}. The currents i_{ds} and i_{qs} can be measured, however, the φ_{ds} and φ_{qs} observer can be calculated from (5) and (6). Furthermore, let the errors be $e_T \equiv u_{Tref} - u_T$ and $e_\phi \equiv u_{\phi ref} - u_\phi$, where u_{Tref} and $u_{\phi ref}$ are the reference values of the active torque and the square of the flux norm. Applying the sliding-mode control theory to the present problem, we first define the integral surface functions for the active torque (s_1) and the square of the flux norm (s_2) as follows:

$$s_1 = e_T + k_1 \int_0^t e_T dt - e_T(0^-) \tag{9}$$

$$s_2 = e_\phi + k_2 \int_0^t e_\phi dt - e_\phi(0^-) \tag{10}$$

where k_1 and k_2 are positive gain. Once the system states stay stationary on the surfaces, we then have $s_1 = s_2 = \dot{s}_1 = \dot{s}_2 = 0$. According to (9) and (10), $\dot{s}_1 = 0$ and $\dot{s}_2 = 0$ lead to

$$\frac{d}{dt}(u_{Tref} - u_T) = -k_1(u_{Tref} - u_T) \tag{11}$$

$$\frac{d}{dt}(u_{\phi ref} - u_\phi) = -k_1(u_{\phi ref} - u_\phi) \tag{12}$$

(11) and (12) ensure that the system states (u_T and u_ϕ) will exponentially converge to the reference values if they are kept on the sliding surfaces $\mathbf{s} = 0$. This condition can be achieved by the sliding-mode control scheme that asks the voltage input $\mathbf{u} = [u_{ds}, u_{qs}]^T$ to drive the state variables of the system to the sliding surface $\mathbf{s} = 0$ and to keep them there. For this purpose, we select the Lyapunov function candidate as

$$V = \frac{1}{2}\mathbf{s}^T\mathbf{s} \tag{13}$$

The time derivative of V needs the derivatives of $\mathbf{s}$. It follows from (1), (2), (9) and (10) that

$$\begin{aligned}\dot{s}_1 =& \dot{e}_T + k_1 e_T \\ =& K_f\left(\frac{R_s}{L_s} i_{qs} + p\omega_r i_{ds} + \frac{p\omega_r}{L_s} K_f\right) + \dot{u}_{Tref} \\ &+ k_1(u_{Tref} - u_T) - \frac{K_f}{L_s} u_{qs}\end{aligned} \tag{14}$$

$$\begin{aligned}\dot{s}_2 =& \dot{e}_\phi + k_2 e_\phi \\ =& L_s R_s m_i + K_f R_s i_{ds} + \dot{u}_{\phi ref} \\ &+ k_2(u_{\phi ref} - u_\phi) - \varphi_{ds} u_{ds} - \varphi_{qs} u_{qs}\end{aligned} \tag{15}$$

or

$$\dot{\mathbf{s}} = \mathbf{b} + \mathbf{D}\mathbf{u} \tag{16}$$

where $\mathbf{b} = [b_1, b_2]^T$ and

$$\mathbf{D} = \begin{bmatrix} 0 & -\frac{K_f}{L_s} \\ -\varphi_{ds} & -\varphi_{qs} \end{bmatrix} \tag{17}$$

in which

$$b_1 = K_f\left(\frac{R_s}{L_s} i_{qs} + p\omega_r i_{ds} + \frac{p\omega_r}{L_s} K_f\right) + \dot{u}_{Tref} + k_1(U_{Tref} - u_T)$$

$$b_2 = L_s R_s m_i + K_f R_s i_{ds} + \dot{u}_{\phi ref} + k_2(u_{\phi ref} - u_\phi)$$

$$m_i = i_{ds}^2 + i_{qs}^2$$

The above equations are derived under the ideal situation. When we consider the uncertainties of the system parameters (e.g., R_s, L_s, K_f) in (1) and (2), then (16) can be directly modified as

$$\begin{aligned}\dot{\mathbf{s}} &= (\mathbf{b} + \Delta\mathbf{b}) + (\mathbf{D} + \Delta\mathbf{D})\mathbf{u} \\ &= \mathbf{b} + \mathbf{z} + \mathbf{D}\mathbf{u}\end{aligned} \tag{18}$$

where $\Delta\mathbf{b}$ and $\Delta\mathbf{D}$ are the uncertainties induced by the model uncertainties in (1) and (2), and

$$\mathbf{z} = \Delta\mathbf{b} + \Delta\mathbf{D}\mathbf{u} \tag{19}$$

Furthermore, we can treat the uncertainty term $\mathbf{z}$ in (19) as a nominal offset value $\mathbf{z}^*$ with a smaller varying uncertainty, i.e., $\mathbf{z} = \mathbf{z}^* + \boldsymbol{\delta}_z$, where $\boldsymbol{\delta}_z = [\delta_{z1}, \delta_{z2}]^T = [z_1 - z_1^*, z_2 - z_2^*]^T$. Then (18) can be rewritten as

$$\dot{\mathbf{s}} = \mathbf{b} + \mathbf{z}^* + \boldsymbol{\delta}_z + \mathbf{D}\mathbf{u} \tag{20}$$

Under the assumption that $\mathbf{z}^*$ and $\boldsymbol{\delta}_z$ are known *a priori*, it can be shown that s_1 and s_2 converge to zero as $t \to \infty$, if the following sliding-mode control law is applied:

$$\mathbf{u} = -\mathbf{D}^{-1}\left(\mathbf{b} + \mathbf{k}_c\mathbf{s} + \begin{bmatrix} \rho_1 \text{sign}(s_1) \\ \rho_2 \text{sign}(s_2) \end{bmatrix} + \mathbf{z}^*\right) \tag{21}$$

where $\boldsymbol{\rho} = [\rho_1, \rho_2]^T$ with $\rho_1 > |\delta_{z1}|$ and $\rho_2 > |\delta_{z2}|$ for all t. (21) exists when the inverse $\mathbf{D}^{-1}$ exists for all time.

However, $\mathbf{z}^*$ and the upper bounds of $\boldsymbol{\delta}_z$ are actually unknown. To get around this difficulty, we can introduce the adaptive sliding-mode control law, which is stated in the following proposition.

***Proposition* 1.** Consider the PMSM in (1) and (2). The overall system will asymptotically converge to $u_T = u_{Tref}$ and $u_\phi = u_\phi$, if the inverse $\mathbf{D}^{-1}$ exists and the following

adaptive sliding-mode controller is applied:

$$\mathbf{u} = -\mathbf{D}^{-1}\left(\mathbf{b} + \mathbf{k}_c\mathbf{s} + \begin{bmatrix}\hat{\rho}_1 \text{sign}(s_1)\\ \hat{\rho}_2 \text{sign}(s_2)\end{bmatrix} + \hat{\mathbf{z}}\right) \tag{22}$$

$$\dot{\hat{\boldsymbol{\rho}}} = \begin{bmatrix}\dot{\hat{\rho}}_1\\ \dot{\hat{\rho}}_2\end{bmatrix} = \begin{bmatrix}|s_1|\\ |s_2|\end{bmatrix} \tag{23}$$

$$\dot{\hat{\mathbf{z}}} = \mathbf{s} \tag{24}$$

Note that $\hat{\boldsymbol{\rho}}$ and $\hat{\mathbf{z}}$ are, respectively, the estimates of $\boldsymbol{\rho}$ and $\mathbf{z}^*$.

The details of proof can be found in the Appendix Section 8.

4 Position control

4.1 Model reference adaptive control

In practical applications of a PMSM, a cascade control structure is suggested: the inner loop is the above described adaptive sliding-mode torque control, while the outer loop can be a speed or position control. Here, we consider only the position control, since the speed control is a simple extension.

The real system to be considered is a single-link mechanical system driven by a PMSM. The block diagram in Fig. 1 illustrates the overall system of the proposed control method, in which the torque and flux estimator are calculated by (7) and (8). Many control methods can be used for the outer loop position controller. We select the model reference adaptive control (MRAC) scheme, because it is one of the most popular adaptive control strategies and it can adapt itself to the unknown mechanical parameters. The position controller generates the torque command to the inner loop controller, which then asks the inverter to provide the required three-phase voltages for the PMSM.

The mechanical system is a PMSM with a rod fixed on the shaft axis of the motor and is shown in Fig. 2. The mechanical model of the system is

$$\begin{aligned} J\ddot{\theta}_m &= -B\dot{\theta}_m - mgl\sin(\theta_m + \theta_0) + k_T u_T \\ &= -B\dot{\theta}_m - mgl\cos\theta_0 \sin\theta_m \\ &\quad - mgl\sin\theta_0\cos\theta_m + k_T u_T \end{aligned} \tag{25}$$

where θ_m is the angular displacement of the shaft, J is the inertia of the motor, B is the friction coefficient, m is the mass of the rod, l is the distance from the shaft center to the center of mass of the rod, g is the gravitational acceleration, k_T is the torque constant, and θ_0 is the null angle from the line of gravity. For the development of the MRAC, (25) is rewritten as

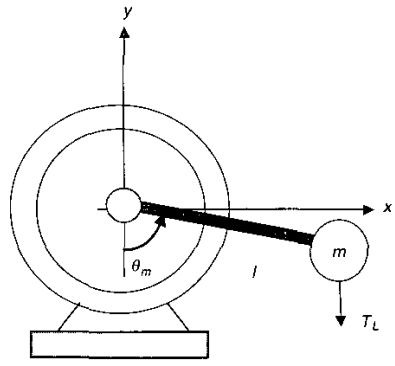

Fig. 2 *Mechanical system of a motor with a rod fixed on the shaft*

$$\ddot{\theta}_m = -B_J\dot{\theta}_m - (L_b\sin\theta_m + L_c\cos\theta_m) + K_J u_T \tag{26}$$

where $B_J = B/J$, $L_b = mgl\cos\theta_0/J$, $L_c = mgl\sin\theta_0/J$, $K_J = k_T/J$. Note that $J>0$.

The reference model of the MRAC is given as

$$\begin{aligned} \ddot{\theta}_m^* &= -k_t\dot{\theta}_m^* - k_s\theta_m^* + k_s r \\ &= -k_t\dot{\theta}_m^* - k_s(\theta_m^* - r) \end{aligned} \tag{27}$$

where θ_m^* is the response of reference angular displacement for an angular displacement command r, k_t, and k_s are so selected that $s^2 + k_t s + k_s = (s+p_1)(s+p_2)$ with $p_1, p_2 > 0$.

We first need to know the model reference control (MRC) law, which can make the overall system asymptotically track the reference model under the assumption that the mechanical parameters are exactly known. The MRC of the present system is

$$u_T = \begin{bmatrix}c_3^*\\ c_2^*\\ c_1^*\\ c_0^*\end{bmatrix}^T \begin{bmatrix}\dot{\theta}_m\\ \sin\theta_m\\ \cos\theta_m\\ r - \theta_m\end{bmatrix} \equiv \mathbf{c}^{*\mathrm{T}}\mathbf{w} \tag{28}$$

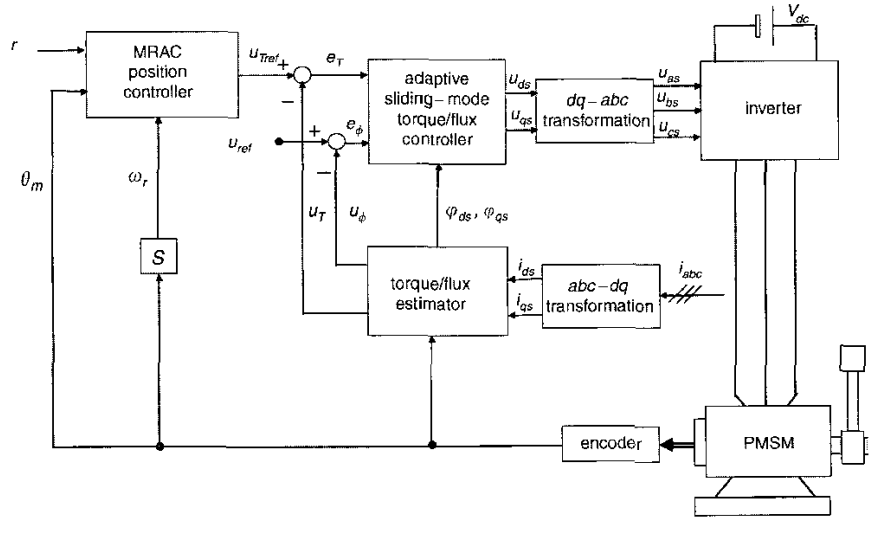

Fig. 1 *Overall system of the position control of a PMSM*

with

$$\mathbf{c}^* = \begin{bmatrix} c_3^* \\ c_2^* \\ c_1^* \\ c_0^* \end{bmatrix} = \begin{bmatrix} (B_J - k_t)/K_J \\ L_b/K_J \\ L_c/K_J \\ k_s/K_J \end{bmatrix} \tag{29}$$

For the case when the parameters are unknown, the MRAC directly follows from MRC by applying adaptive laws to the estimation of the system parameters. We use the direct MRAC with unnormalized adaptive laws [19]. Since the system has the relative degree of 2, we need the bilinear parametric model of the position error $e \equiv \theta_m - \theta_m^*$. Substituting $u_T = \mathbf{c}^{\mathrm{T}}\mathbf{w} + (u_T - \mathbf{c}^{\mathrm{T}}\mathbf{w})$ into (26) and combining (27), we obtain $(s^2 + k_v s + k_s)e = K_J(u_T - \mathbf{c}^{\mathrm{T}}\mathbf{w})$, which turns out to be the bilinear parametric model:

$$e = W_m(s)\rho^* \left(\frac{u_T}{s + p_1} - \mathbf{c}^{*\mathrm{T}}\overline{\mathbf{w}} \right) \tag{30}$$

where $W_m(s) = k_s/(s + p_2)$, $\rho^* = K_J/k_s$, and $\overline{\mathbf{w}} = \mathbf{w}/(s + p_1)$.

According to Table 6.2 in [18], we then propose the MRAC for (30) as follows:

$$u_T = \hat{\mathbf{c}}^{\mathrm{T}}\mathbf{w} + \dot{\hat{\mathbf{c}}}^{\mathrm{T}}\overline{\mathbf{w}} \tag{31}$$

with

$$\dot{\overline{\mathbf{w}}} = -p_1\overline{\mathbf{w}} + \mathbf{w}, \quad \overline{\mathbf{w}}(0) = 0 \tag{32}$$

and the adaptive laws

$$\dot{\hat{\mathbf{c}}} = -\Gamma e\overline{\mathbf{w}}\,\mathrm{sign}(\rho^*) \tag{33}$$

where Γ is a diagonal matrix with positive diagonal entries. It should be remarked that the sign of ρ^* is always known.

4.2 Experiments

The overall position control scheme in Fig. 1 will be verified by experiments. The experimental system is shown in Fig. 3, which is a PC-based control system. A servo control card on the ISA bus of the PC provides eight A/D converters, four D/A converters, and an encoder counter. The inner loop and the outer loop controllers are implemented on the PC in C-language. The sampling time for the overall control is 0.3 ms. The ramp comparison modulation circuit is used to generate the PWM for driving the IGBT module inverter. The PMSM in the experimental system is a 4-pole, 200 W, and 92 V motor with the rated current, speed, and torque of 2.2 A, 3000 rpm, and 0.5 Nm, respectively. The encoder has 2000 counters per revolution. The parameters of the motor are $R_s = 2.14\,\Omega$, $L_s = 2.4\,mH$, and $K_f = 0.0738$. Those of the mechanical system (see Fig. 2) are $J \approx 0.00042\,kgm^2$, $l \approx 0.1\,m$, and $m \approx 0.5\,kg$.

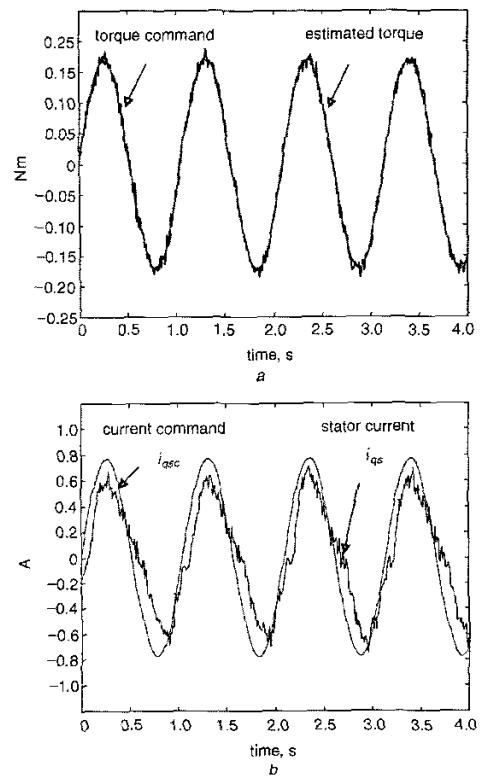

Fig. 4 *Responses of a sinusoidal torque command*
a Adaptive sliding-mode torque control scheme
b RFO current control scheme

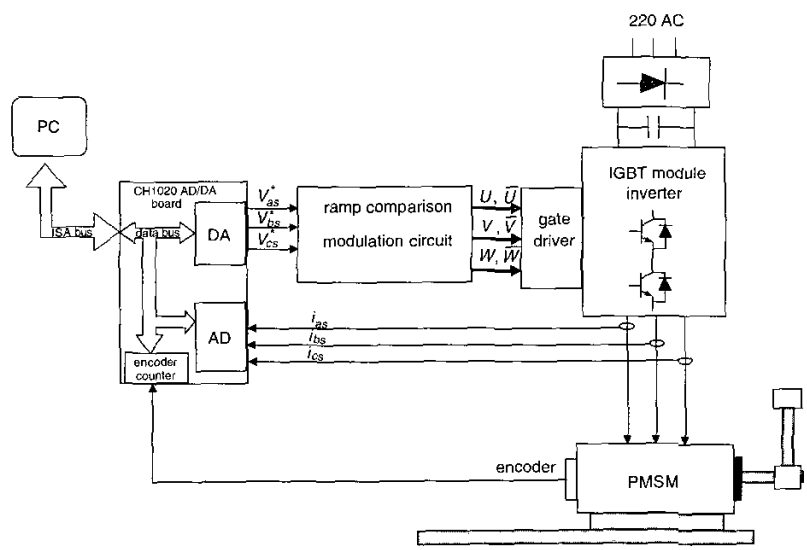

Fig. 3 *Experimental system*

Three experiments are conducted: 1) torque tracking control, 2) set-point position control, and 3) position tracking control. The gains of the reference model (27) are $k_t = 30$ and $k_s = 225$. The popular rotor field-oriented (RFO) control scheme is also established to a performance comparison.

In the first experiment, we consider only the inner torque control loop given as $u_T = 0.06\sin(1.8\pi t)$. The experimental results for the proposed controller and the RFO are shown in Figs. 4 and 5. It is apparent that the proposed controller is superior to the conventional RFO controller for the sinusoidal torque tracking. When the motor speed is high, the term $(pK_f/L_s)\omega_r$ makes the motor model far from the linearised system, so that the linear PI controller in the RFO can no longer compensate for the large nonlinearity.

In the second experiment, the motor is asked to go to $\theta_m = \pi$ at $t = 0$ s, and then to return to $\theta_m = \pi/2$ at $t = 2$ s. It should be noted that the reference active torque u_{Tref} is generated by the MRAC and varies before the steady-state is reached, while the reference square flux $u_{\phi ref}$ is given as a constant. The experimental results of both controllers are shown in Figs. 6–11. The transient response of the proposed controlled is enlarged and shown in Figs. 12 and 13. It can be seen that the steady-state error is negligible. The history of the estimated torque shows that the values are around zero for $\theta_m = \pi$ and around about 0.5 Nm for $\theta_m = \pi/2$, which is consistent with the physical property. Fig. 6*b* shows that the parameters of the MRAC also converge to constant values, which is a property of the MRAC. It is seen from Fig. 7*b* that there is fluctuation in the estimated torque. This oscillation comes from the oscillation of the currents, because the estimated torque is computed using the measured currents. This oscillation does not affect the

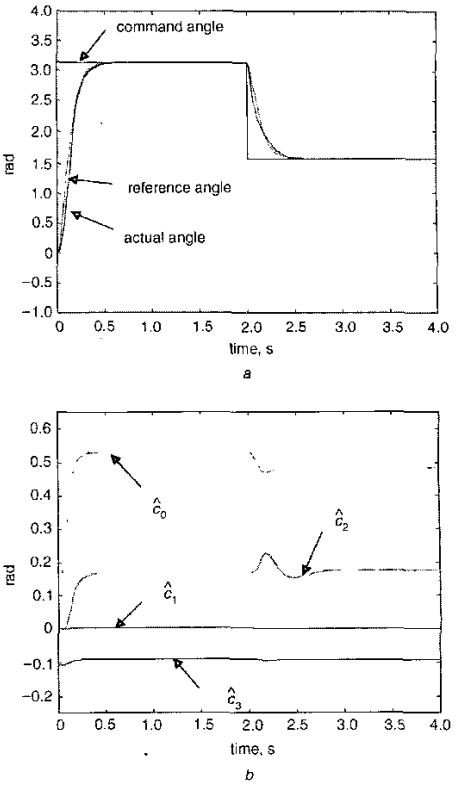

Fig. 6 *Responses of a set point position command*
a Position
b Estimated parameters

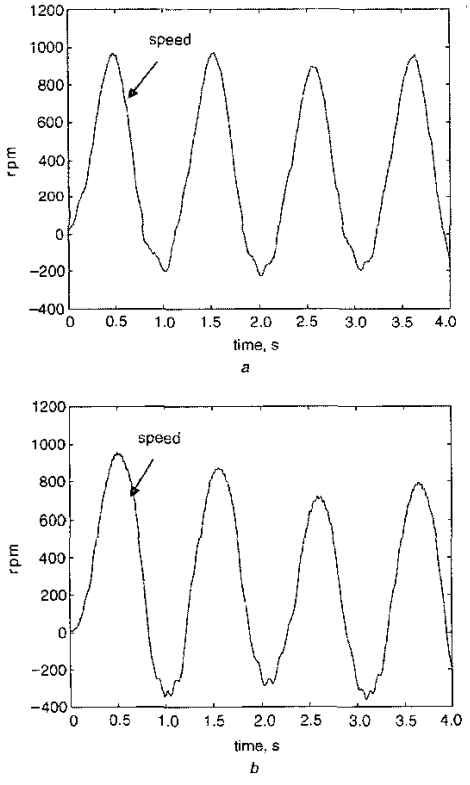

Fig. 5 *Responses of a sinusoidal torque command*
a Speed of adaptive sliding-mode torque control scheme
b Speed of RFO current control scheme

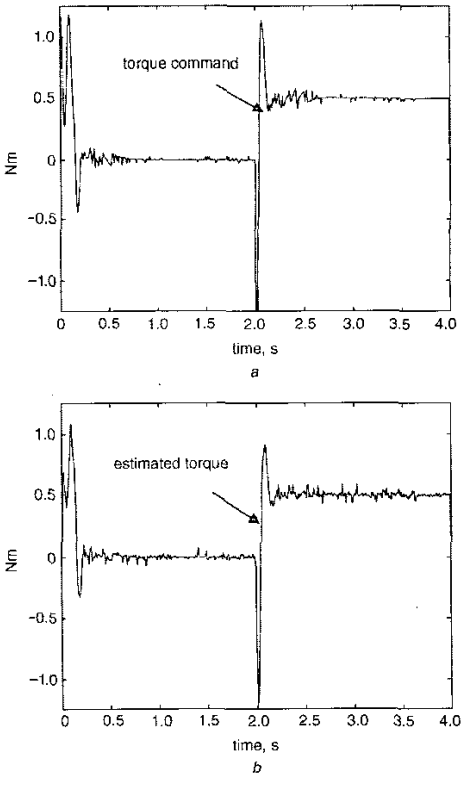

Fig. 7 *Responses of a set point position command*
a Torque command
b Estimated torque

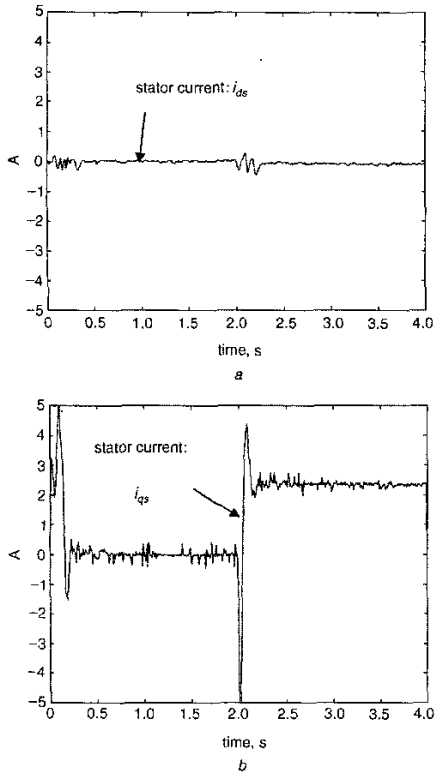

Fig. 8 *Responses of a set point position command*
a Stator current (i_{ds})
b Stator current (i_{qs})

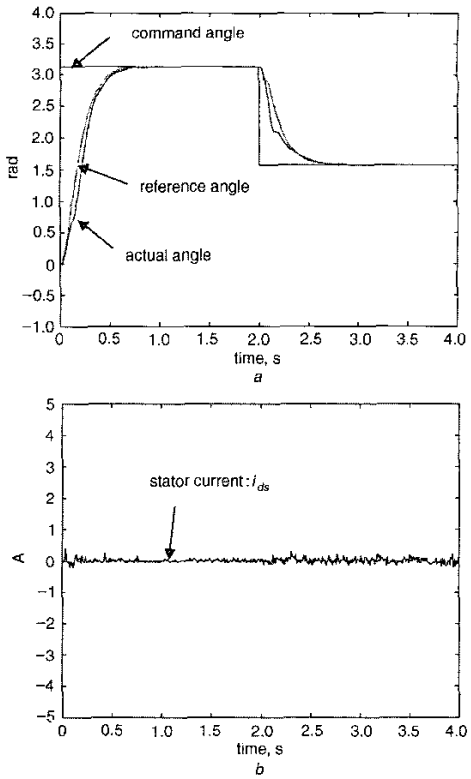

Fig. 10 *Response of a set point command with RFO current control scheme*
a Position *b* Stator current (i_{ds})

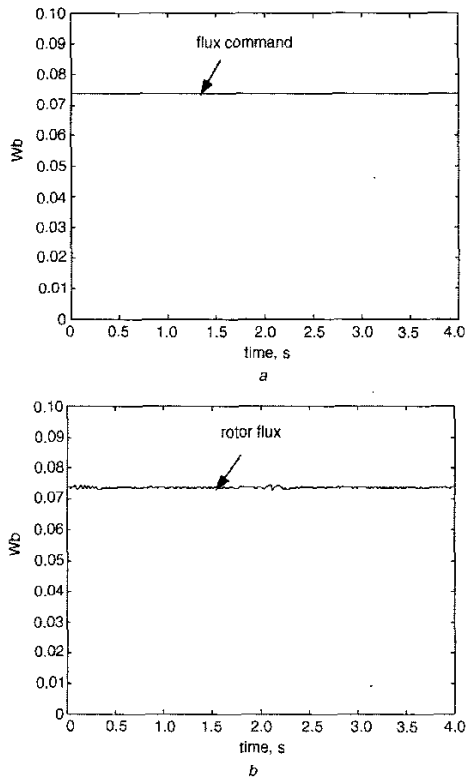

Fig. 9 *Responses of a set point position command*
a Command flux
b Estimated rotor flux

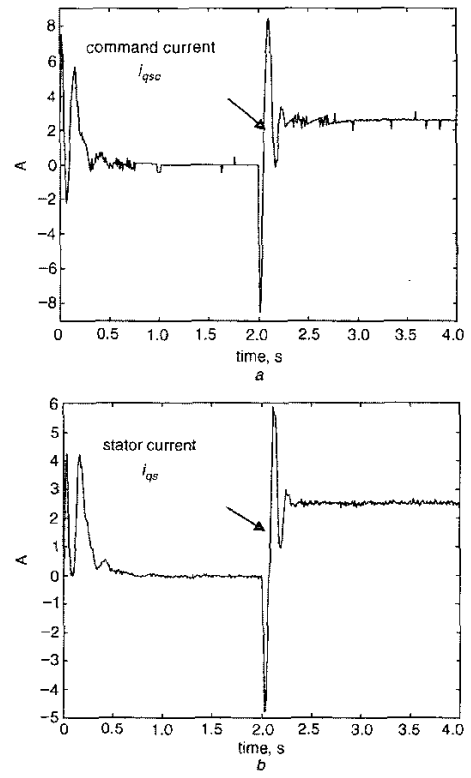

Fig. 11 *Response of a set point command with RFO current control scheme*
a Command current (i_{qsc}) *b* stator current (i_{qs})

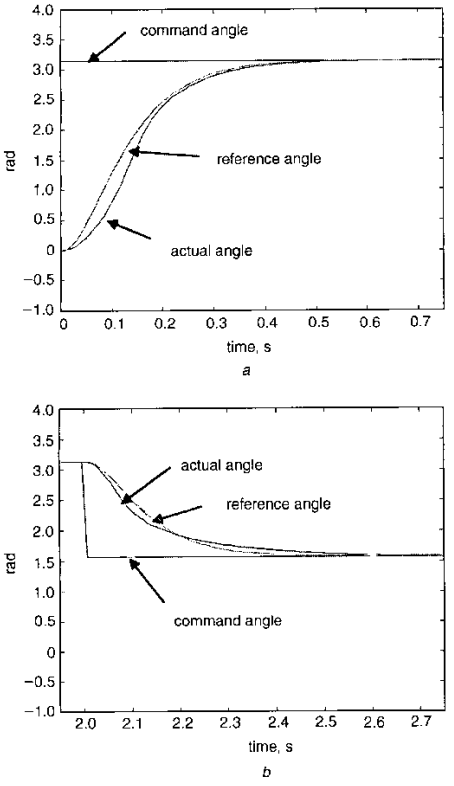

Fig. 12 *Transient parts of Figs. 6–9*
a Position response for 0 ~ 0.75 s
b Position response for 1.95 ~ 2.75 s

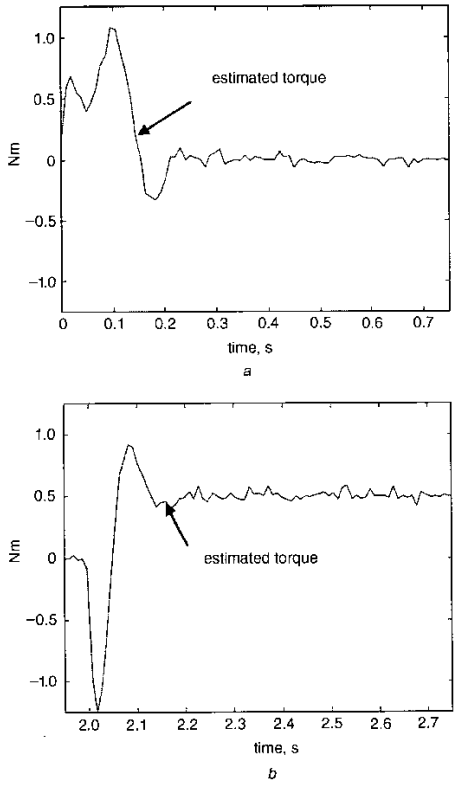

Fig. 13 *Transient parts of Figs. 6–9*
a Estimated torque response for 0 ~ 0.75 s
b Estimated torque response for 1.95 ~ 2.75 s

output of the mechanical system, since its frequency is far from the bandwidth of the mechanical system. The comparison of Figs. 6–9 with Figs. 10 and 11 shows that the performance of both controller is equally good.

In the third experiment, a sinusoidal position command is given as

$$r = (1 - e^{-10t})^2 \frac{\pi}{2} \sin(3\pi t) \tag{34}$$

which makes the starting smooth, since $\dot{\omega}_r^*(0) = \omega_r^*(0) = \theta_m = 0$. The experimental results of both controllers are shown in Figs. 14–17. Although there is a delay between the response θ_m and the command r, the tracking error $\theta_m - \theta_m^*$ is actually negligible for the proposed controller, but is noticable small for the RFO. Although both controllers have almost the same performance for the position regulation, the proposed controller has good torque tracking and good position tracking, whereas the RFO has significant error in the torque tracking, so that also has some noticable errors in the position tracking.

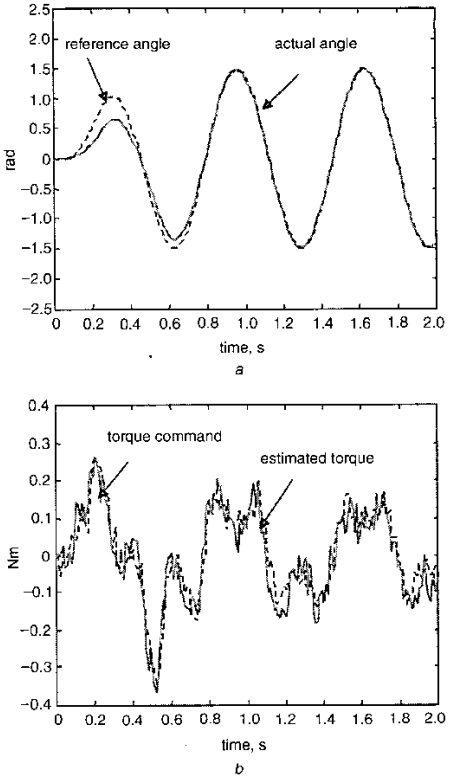

Fig. 14 *Responses of a sinusoidal position command with adaptive sliding-mode torque control scheme*
a Position
b Torque command and estimated torque

5 Conclusions

This paper presents a new adaptive sliding-mode torque control for a PMSM. The sliding-mode controller is constructed by two integral surface functions. We also use the concept of the adaptive sliding-mode control to handle the uncertainty. The proposed control scheme is formulated in Proposition 1. To demonstrate the usefulness of the torque control scheme, we applied it to the position control of a PMSM. The overall control system is a cascade structure with the torque control as the inner loop and the

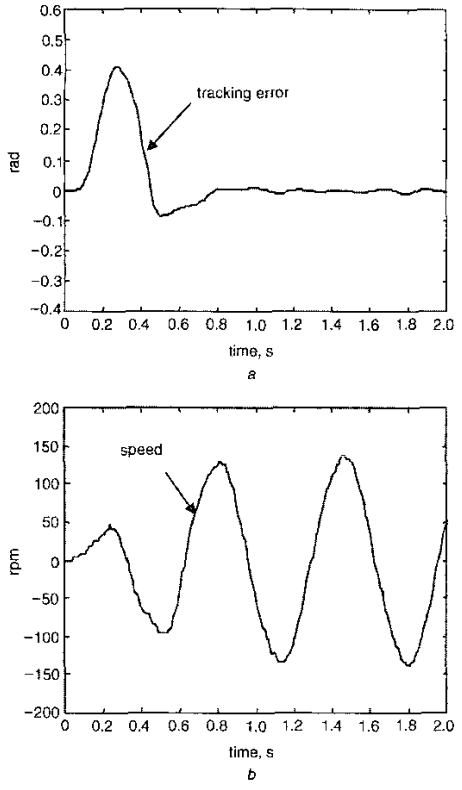

Fig. 15 *Responses of a sinusoidal position command with adaptive sliding-mode torque control scheme*
a Tracking error $(\theta_m - \theta_m^*)$ *b* Speed

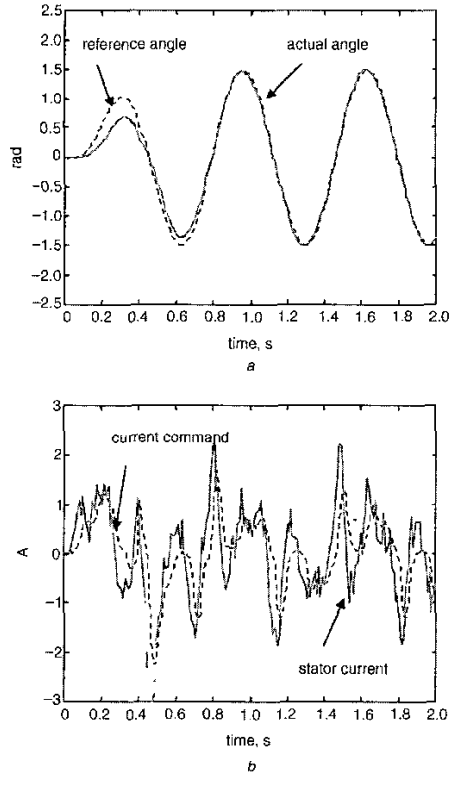

Fig. 16 *Responses of a sinusoidal position command with RFO current control scheme*
a Position *b* Current command (i_{qsc}) and estimated current (i_{qs})

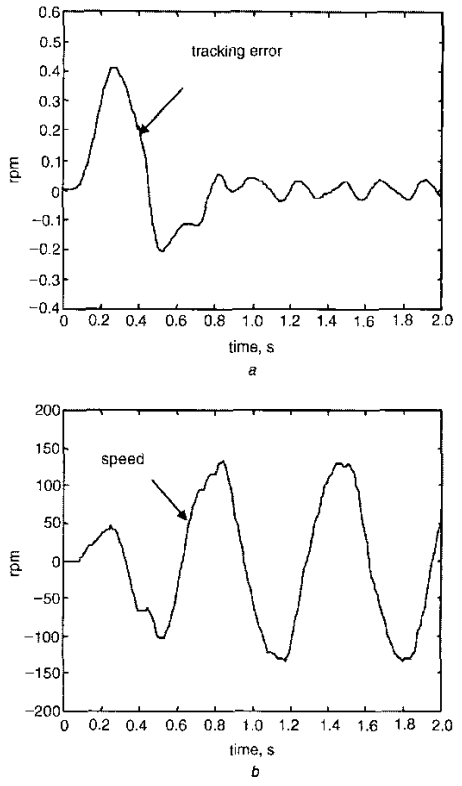

Fig. 17 *Responses of a sinusoidal position command with RFO current control scheme*
a Tracking error $(\theta_m - \theta_m^*)$
b Speed

MRAC as the outer loop. The control system is implemented on a PC-based system to control a motor with a rod fixed on the shaft. Both set-point and tracking position control experiments verified the control theory and showed that the proposed control scheme is useful for industrial applications. Furthermore, a comparison with the conventional RFO controller is also presented. Since the application of a PM machine to the field weakening condition is difficult, the proposed controller is not recommended for high-speed motion.

6 Acknowledgment

This paper was in part supported by the National Science Council, Taiwan under Grant No. NSC89-2213-E-009-216.

7 References

1 NEE, H.P., LEFEVRE, L., THELIN, P., and SOULARD, J.: 'Determination of d and q reactance of permanent-magnet synchronous motors without measurements of the rotor position', *IEEE Trans. Ind. Appl.*, 2000, **36**, (5), pp. 1330–1335
2 KAZMIERKOWSKI, M.P., and MALESANI, L.: 'Current control technique for three phase voltage-source PWM converters: a survey', *IEEE Trans. Ind. Electron.*, 1998, **45**, (5), pp. 691–703
3 HOANG, L.H., KAPIM, S., and PHILIPPE, V.: 'Analysis and implementation of a real-time predictive current controller for permanent-magnet synchronous servo drives', *IEEE Trans. Ind. Electron.*, 1994, **41**, (1), pp. 110–117
4 KIM, K.H., BAIK, I.C., and YOUN, M.J.: 'An improved digital current control of a PM synchronous motor with a simple feedforward disturbance compensation scheme', *Proceedings of IEEE Power Electronics Specialists Conference*, 1998, pp. 101–107
5 KUKRER, O.: 'Discrete-time current control of voltage-fed three-phase PWM inverters', *IEEE Trans. Power Electron.*, 1996, **11**, pp. 260–269

6 NOVOTNY, D.W., and LIPO, T.A.: 'Vector control and dynamics of AC drives', (Oxford, New York, 1996)
7 ZHONG, L., RAHMAN, M.F., HU, W.Y., and LIM, K.W.: 'Analysis of direct torque control in permanent magnet synchronous motor drives', *IEEE Trans. Power Electron.*, 1997, **12**, pp. 528–536
8 LUUKKO, J., and PYRHONEN, J.: 'Selection of the flux linkage reference in a direct torque controlled permanent magnet synchronous motor drive', *AMC'98*, 1999, pp. 198–203
9 ZOLGHADRI, M.R., GAIRAUD, J., DAVOINE, J., and ROYE, D.: 'A DSP based direct torque controller for permanent magnet synchronous motor drives', *Proceedings of IEEE Power Electronics Specialists Conference*, 1998, pp. 2056–2061
10 TAKAHASHI, I., and NOGUCHI, T.: 'A new quick-response and high-efficiency control strategy of an induction motor', *IEEE Trans. Ind. Appl.*, 1986, **22**, pp. 820–827
11 SOLSONA, J., VALLA, M.I., and MURAVCHIK, C.: 'Nonlinear control of a permanent magnet synchronous motor with disturbance torque estimation', *IEEE Trans. Electromagr. Compat.*, 2000, **15**, pp. 163–168
12 BAIK, I.C., KIM, K.H., and YOUN, M.J.: 'Robust nonlinear speed control of PM synchronous motor using boundary layer integral sliding mode control technique', *IEEE Trans. Control Syst. Technol.*, 2000, **8**, pp. 47–54
13 LIN, F.J., and CHIU, S.L.: 'Adaptive fuzzy sliding-mode control for PM synchronous servo motor drives', *IEE Proc. Control Theory Appl.*, 1998, **145**, (1), pp. 63–72
14 CHEN, J., and TANG, P.C.: 'A sliding mode current control scheme for PWM brushless DC motor drives', *IEEE Trans. Power electron.*, 1999, **14**, pp. 541–550
15 CHUNG, S.K., LEE, J.H., KO, J.S., and YOUN, M.J.: 'Robust speed control of brushless direct-drive motor using integral variable structure control', *IEE Proc. Electr. Power Appl.*, 1995, **142**, (6), pp. 361–370
16 YU, H., and LIOYD, S.: 'Variable structure adaptive control of robot manipulators', *IEE Proc. Control Theory Appl.*, 1997, **144**, (2), pp. 167–176
17 CHEN, H.C., HUANG, M.S., LIAW, C.M., CHANG, Y.C., YU, P.Y., and HUANG, J.M.: 'Robust current control for brushless DC motors', *IEE Proc. Electr. Power Appl.*, 2000, **147**, (6), pp. 503–512
18 VAS, P.: 'Vector control of AC machines', (Clarendon Press, 1996)
19 IOANNOU, P.A., and SUN, J.: 'Robust adaptive control', (Prentice-Hall, New Jersey, 1996)
20 KHAIL, H.K.: 'Nonlinear systems', (Prentice-Hall, New Jersey, 1996)

8 Appendix

Proof of proposition 1. Define the Lyapunov-like function as

$$V = \frac{1}{2}(\mathbf{s}^2 + \tilde{\boldsymbol{\rho}}^2 + \tilde{\mathbf{z}}^2) \tag{35}$$

where $\tilde{\boldsymbol{\rho}} = \hat{\boldsymbol{\rho}} - \boldsymbol{\rho}$, $\tilde{\mathbf{z}} = \tilde{\mathbf{z}} - \mathbf{z}^*$. It follows from (20) and (22) that

$$\begin{aligned} \dot{V} &= \mathbf{s}^T\dot{\mathbf{s}} + \tilde{\boldsymbol{\rho}}^T\dot{\hat{\boldsymbol{\rho}}} + \tilde{z}^T\dot{\tilde{\mathbf{z}}} \\ &= -\mathbf{s}^T(\mathbf{k_c}\dot{\mathbf{s}} + \tilde{\mathbf{z}}) + \mathbf{s}^T\boldsymbol{\delta}_\mathbf{z} \\ &\quad - (\hat{\rho}_1|s_1| + \hat{\rho}_2|s_2|) + \tilde{\boldsymbol{\rho}}^T\dot{\hat{\boldsymbol{\rho}}} + \tilde{\mathbf{z}}^T\dot{\tilde{\mathbf{z}}} \\ &\leq -\mathbf{s}^T(\mathbf{k_c}\dot{\mathbf{s}} + \tilde{\mathbf{z}}) - (\hat{\rho}_1|s_1| + \hat{\rho}_2|s_2|) \\ &\quad + \tilde{\boldsymbol{\rho}}^T\dot{\hat{\boldsymbol{\rho}}} + \tilde{\mathbf{z}}^T\dot{\tilde{\mathbf{z}}} = -\mathbf{s}^T(\mathbf{k_c}\dot{\mathbf{s}} + \tilde{\mathbf{z}}) \leq 0 \end{aligned} \tag{36}$$

Note that $(\rho_1|s_1| + \rho_2|s_2| \geq \mathbf{s}^T\boldsymbol{\delta}_\mathbf{z}$. The last equality in (36) is obtained by applying the adaptive laws (23) and (24).

The fact that V is bounded below and nonincreasing implies that $\lim_{t\to\infty} V = V_\infty$ exists [20]. Thus, $\mathbf{s}$, $\tilde{\boldsymbol{\rho}}$, $\tilde{\mathbf{z}} \in L_\infty$, which implies that $\hat{\boldsymbol{\rho}}$, $\hat{\mathbf{z}} \in L_\infty$ since $\boldsymbol{\rho}$ and $\mathbf{z}^*$ are constants. It then follows from (20) and (22) that $\dot{\mathbf{s}} \in L_\infty$. Integrating (36), we obtain $V_0 - V_\infty \geq \int_0^\infty \mathbf{s}^\mathbf{T}\mathbf{k_c}\mathbf{s}$, and $\mathbf{s} \in L_2$. A corollary of Barbalat's lemma [20] states that $\dot{\mathbf{s}} \in L_\infty$ and $\mathbf{s} \in L_2$ implying $\mathbf{s} \to 0$ as $t \to \infty$. This completes the proof. **Q.E.D.**

***Remark* 1.** The restriction of the existence of the inverse $\mathbf{D}^{-1}$ is easily satisfied. According to (17), $\mathbf{D}$ is nonsingular if and only if φ_{ds} is nonzero. The constraint of $\varphi_{ds} > 0$ will be satisfied if the initial value is greater than zero. Nevertheless, in the implementation φ_{ds} is replaced with a small value of ε if $\varphi_{ds} < \varepsilon$.

The undesirable chattering of sliding-mode techniques can be remedied by replacing switching function sign (s_i) by the saturation function

$$Sat(s_i) = \frac{s_i}{|s_i| + \lambda} \tag{37}$$

where $\lambda > 0$ is a smoothing factor. ■